ELSEVIER

Chemical Engineering Journal 112 (2005) 45–55

Chemical Engineering Journal

www.elsevier.com/locate/cej

Mixing mechanism in a modified co-current downflow bubble column

Subrata Kumar Majumder*, Gautam Kundu, Dibyendu Mukherjee

Department of Chemical Engineering, Indian Institute of Technology, Kharagpur 721302, India

Received 19 February 2005; received in revised form 12 June 2005; accepted 17 June 2005

Abstract

Experimental measurements of longitudinal dispersion coefficients of liquid have been carried out in an ejector-induced bubble column operating with co-current downflow of gas and liquid. The experimental data obtained show that the hydrodynamics of the bubble column depend on nozzle diameter, liquid jet velocity and superficial liquid and gas velocities. A model with the consideration of combined action of velocity profile and the bubble motion was developed from Taylor's theory. The dispersion coefficient of bubble motion, D_b, and the characteristic factor of velocity distribution, k, depends on the nozzle diameter, fluid velocities, which give the corresponding model equations. The dispersion coefficient calculated from the model shows a good agreement with the experimental data of this investigation in the ejector-induced downflow bubble column.

Keywords: Downflow bubble column; Liquid jet; RTD; Dispersion coefficient

1. Introduction

Bubble columns find numerous applications in the process industry due to their relatively simple construction, low operating costs, excellent heat transfer characteristics to immersed surfaces and the ease with which, the liquid residence time can be varied. However, many important fluid dynamical aspects of the prevailing gas–liquid two-phase flows are still poorly understood, despite their frequent use in variety of industrial processes. This is mainly due to the difficulty in understanding the complex flow fields in bubble columns and the relation between the flow pattern and design parameters such as pressure drop, fractional gas hold-up and liquid-phase mixing.

A lot of studies have been reported on the hydrodynamics of two-phase co-current flow in bubble columns but the majority of these studies deal with either horizontal two-phase flow or vertical two-phase up flow. Reports on two-phase vertical downflow in bubble columns are scanty. These studies can be categorized either under a plunging jet or sparger-type system. In the plunging jet system, a jet of liquid while plunging into a pool of the same liquid carries along with it some ambient gas, which disperses into bubbles due to momentum transfer of the jet. The liquid and gas bubbles move down through the liquid pool to some distance and the gas bubbles then move up. In the sparger-type system, gas is allowed to pass through the sparger and the liquid flowing past the sparger shears the gas and carries it down the column. In the gas–liquid ejector-induced co-current downflow bubble column reactor, both gas and liquid are concentrically introduced and the kinetic energy of the liquid jet is utilized to disperse gas into fine bubbles. Recently, this type of reactor has earned greater attention in industrial applications which make full use of the advantages of its finer and uniform bubble size, homogenization of the two phases, higher dispersion efficiency and higher residence time of gas bubbles, large interfacial areas and mass transfer rates. Some of the relevant work that have been published [3–5,8,14,15,17,18] are relevant to the liquid jet ejector systems.

Good knowledge of the extent of longitudinal mixing in the liquid phase is essential for the modeling, design and optimization of bubble column. Several studies have been done to account the mixing characteristics by residence time distribution techniques. Towell and Ackerman [27] studied

* Corresponding author. Tel.: +91 3222 281375; fax: +91 3222 282250.
E-mail address: rsmaju@yahoo.com (S.K. Majumder).

1385-8947/$ – see front matter © 2005 Elsevier B.V. All rights reserved.
doi:10.1016/j.cej.2005.06.006

Nomenclature

A_c	cross-sectional area of column (m^2)
A_n	cross-sectional area of nozzle (m^2)
C	tracer concentration of collected sample at time t (kg/m^3)
C_0	input tracer concentration (kg/m^3)
C_θ	normalized concentration (C/C_0)
D_b	diffusion coefficient of bubble motion (m^2/s)
D_C	diameter of the column (m)
D_m	molecular diffusion coefficient in liquid phase (m^2/s)
D_n	diameter of the nozzle (m)
D_T	diameter of tube (m)
E_z	longitudinal dispersion coefficient (m^2/s)
g	gravitational acceleration (m/s^2)
H	clear liquid height (m)
H_0	level of the bubbly flow (m)
k	characteristic factor of velocity distribution, dimensionless
ΔP	pressure drop (N/m^2)
Pe	Peclet number, dimensionless
Q_L	liquid flowrate (m^3/s)
Q_G	gas flowrate (m^3/s)
RTD	residence time distribution
R^2	correlation coefficient, dimensionless
t	time (s)
t_m	mean residence time (s)
V_G	interstitial gas velocity $[V_{SG}/\varepsilon_G]$ (m/s)
V_j	liquid jet velocity $[Q_L/A_n]$ (m/s)
V_L	interstitial liquid velocity $[V_{SL}/(1-\varepsilon_G)]$ (m/s)
V_{L0}	interstitial liquid velocity in the centerline of the column
V_{SG}	superficial gas velocity $[Q_G/A_C]$ (m/s)
V_{SL}	superficial liquid velocity $[Q_L/A_c]$ (m/s)
V_0	representative local velocity defined in Eq. (6) (m/s)
X	parameter defined in Eq. (15)
Z	axial length (m)
Z_e	effective column length (m)

Greek letters

ε_G	fractional gas hold-up, dimensionless
μ_L	viscosity of the liquid (kg/(m s))
θ	dimensionless time (t/t_m), dimensionless

the axial mixing of liquid and gas in large bubble reactors with air–water system. They reported that the axial dispersion coefficient vary with the column diameter and the superficial gas velocity. Hikita and Kikukawa [11] studied the liquid-phase mixing on upflow bubble column reactor. They reported that not only column diameter and gas velocity effect the liquid dispersion but also the viscosity of the liquid has strong effect on the intensity of liquid-phase dispersion. Deckwer et al. [7] determined the liquid dispersion coefficient by stationary and a transient method in co-current bubble columns (15 and 20 cm diameter, 440 and 723 cm high) with different gas distributors. Ogawa et al. [21] studied the liquid-phase mixing in the upward gas–liquid jet reactor with liquid jet ejector. The longitudinal liquid-phase mixing pattern was quite different between the spouting section and the calm section. Groen et al. [9] investigated the axial dispersion phenomena in homogeneously aerated air–water bubble columns. They reported that axial dispersion in bubble column is regarded as transport with a typical velocity over a typical distance. They also proposed a model defining the axial dispersion coefficient as the product of the typical velocities with the column diameter which agrees well with existing literature data at lower superficial gas velocity conditions. Zahradník and Fialová [30] studied the extent of axial mixing in gas and liquid phases in tall upflow bubble column reactors with bubbling regimes. The experimental results proved an essential effect of gas dispersion mode (bubbling regime) on the extent of gas and liquid-phase mixing in the reactor. They also obtained the respective dependences of Peclet number of both gas and liquid on the superficial gas velocity. Hebrard et al. [10] studied axial liquid mixing in sparger-type upflow bubble columns and in membrane and perforated plate bubble columns. They observed that gas sparger has a strong effect on the gas flow regime and consequently on the axial liquid mixing. Krishna et al. [13] developed a reliable correlation for the liquid-phase longitudinal dispersion coefficient in upflow bubble column reactors. The measurements were performed in the churn-turbulent regime of operation with superficial gas velocities in the range 0.05–0.35 m/s. Ahmad [1] studied liquid axial dispersion and gas hydrodynamics in water–air upflow bubble column under slug flow conditions. In contrast to results reported by other investigators, his study showed that the liquid superficial velocity had significant effect on the longitudinal dispersion coefficient. Several other studies regarding mixing in bubble column have been reported by different authors [19,22,24,25,28,29].

Recently, downflow bubble column reactor with ejector-type of gas–liquid distributor for improved gas–liquid mixing, have been recommended for many industrial processes like absorption, desorption and scrubbing, gas–liquid reactions, aerobic fermentations, waste treatment, etc. Therefore, a precise knowledge of the hydrodynamics, mixing characteristics and mass transfer characteristics of the two phase in downflow bubble column, forming a part of an ejector system is of considerable interest.

From the literature, it is observed that there have been no reliable studies regarding the longitudinal mixing made on the ejector-induced downflow bubble column. The purpose of the present study is, therefore, to determine experimentally the longitudinal liquid dispersion coefficient in an ejector-induced downflow bubble column and to develop a model based on the above study. The model considering the combined action of velocity profile and bubble motion has been developed from Taylor's theory.

2. Analysis of mixing

Most of the works concerning the study of liquid-phase dispersion coefficients in bubble column reactor have attempted to characterize the liquid mixing in terms of an overall longitudinal dispersion for the whole reactor. The longitudinal dispersion model is the simplest mathematical description of the flow system in which both convection and diffusion are important. From the analogy between Fick's law for molecular diffusion and the dispersion process, model Eq. (1) can be written for the dispersion phenomenon with the following basic assumptions:

(1) the liquid velocity distribution is uniform;
(2) the bulk flow exists only in the axial direction;
(3) the liquid-phase dispersion exists in axial direction only and the longitudinal dispersion coefficient is independent of spatial co-ordinates;
(4) axis-symmetric tracer concentration distribution exists.

$$\frac{\partial C}{\partial t} = E_z \frac{\partial^2 C}{\partial Z^2} - \frac{V_{SL}}{1-\varepsilon_G}\frac{\partial C}{\partial Z} \tag{1}$$

where the parameter E_z is the longitudinal dispersion coefficient of the liquid phase uniquely characterizing the degree of mixing during the flow. The analytical solution of Eq. (1) for the normalized response curves has been proposed by Ref. [16] by using the open-boundary conditions as follows:

$$C_\theta = \frac{1}{2\sqrt{\pi\theta/Pe}} \exp\left[-\frac{(1-\theta)^2 Pe}{4\theta}\right] \tag{2}$$

where $1/Pe = ((1-\varepsilon_G)E_z/V_{SL}Z_e)$ is called dispersion number, which measures the extent of longitudinal dispersion in the liquid phase, $C_\theta = C/C_0$ and $\theta = t/t_m$ are the dimensionless concentration and time, respectively, C the tracer concentration of collected sample at time t (s) and C_0 is the input tracer concentration. The distance 'Z_e' between the points of tracer injection and the measuring plane has been considered as positive in the direction of flow. A method of moments has been used to estimate the longitudinal dispersion number ($1/Pe$) by the following equation by taking of average of four repeated experiments.

$$\sigma_\theta^2 = \frac{\sigma^2}{t_m^2} = \frac{2}{Pe} + \frac{8}{Pe^2} \tag{3}$$

where t_m and σ were calculated, respectively, as:

$$t_m = \frac{\sum t_i C(t_i)\Delta t_i}{\sum C(t_i)\Delta t_i} \tag{4}$$

$$\sigma^2 = \frac{\sum (t_i - t_m)^2 C(t_i)\Delta t_i}{\sum C(t_i)\Delta t_i} \tag{5}$$

For $Pe = 10.86$ (calculated by Eqs. (3)–(5)), Fig. 1 shows a typical comparison of the experimental data with theoretical Eq. (2) at nozzle diameter 0.006 m and superficial liquid velocity 6.87×10^{-2} m/s and superficial gas velocity 4.71×10^{-3} m/s with a standard deviation 0.322. Longitudinal dispersion coefficient was calculated as $E_z = [V_{SL}Z_e/(1-\varepsilon_G)](1/Pe)$. In this present study, E_z was considered as averaged longitudinal dispersion coefficient over the whole column.

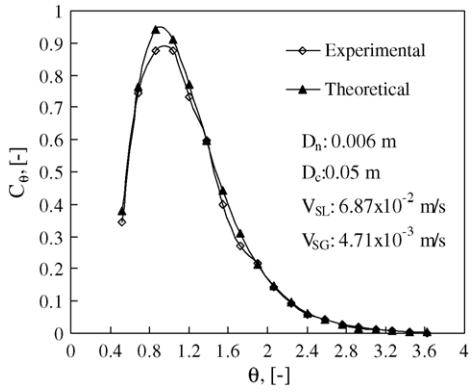

Fig. 1. C_θ vs. θ curve: experimental and predicted.

3. Modeling of mixing mechanism

As shown from the experimental data of the investigation, the dispersion coefficient exhibits mixing performance depending on nozzle diameter, superficial liquid velocity and superficial gas velocity. In this section, a model is developed to interpret the mixing behaviour, which is based on the fluid motion in the bubbly flow.

4. Velocity distribution model

In the condition of bubble flow, liquid flows in the vertical direction with wide distribution of velocities over the cross-section of the column. The mixing of liquid occurs under the combined action of variation of velocity and the motion of gas bubbles in the liquid. This is the basis of the velocity distribution model, which is developed from Taylor's model [26].

5. Model equations

According to Ref. [26], the dispersion of homogeneous system in tube occurred when a solute is transported by a stream of non-uniform velocity. Aris [2] extended Taylor's work by using method of moments and obtained a general form of dispersion coefficient as follows:

$$E_z = \frac{D_T^2 V_0^2}{k D_m} + D_m \tag{6}$$

where D_m and V_0 represent the molecular diffusion coefficient and the maximum velocity at column axis, respec-

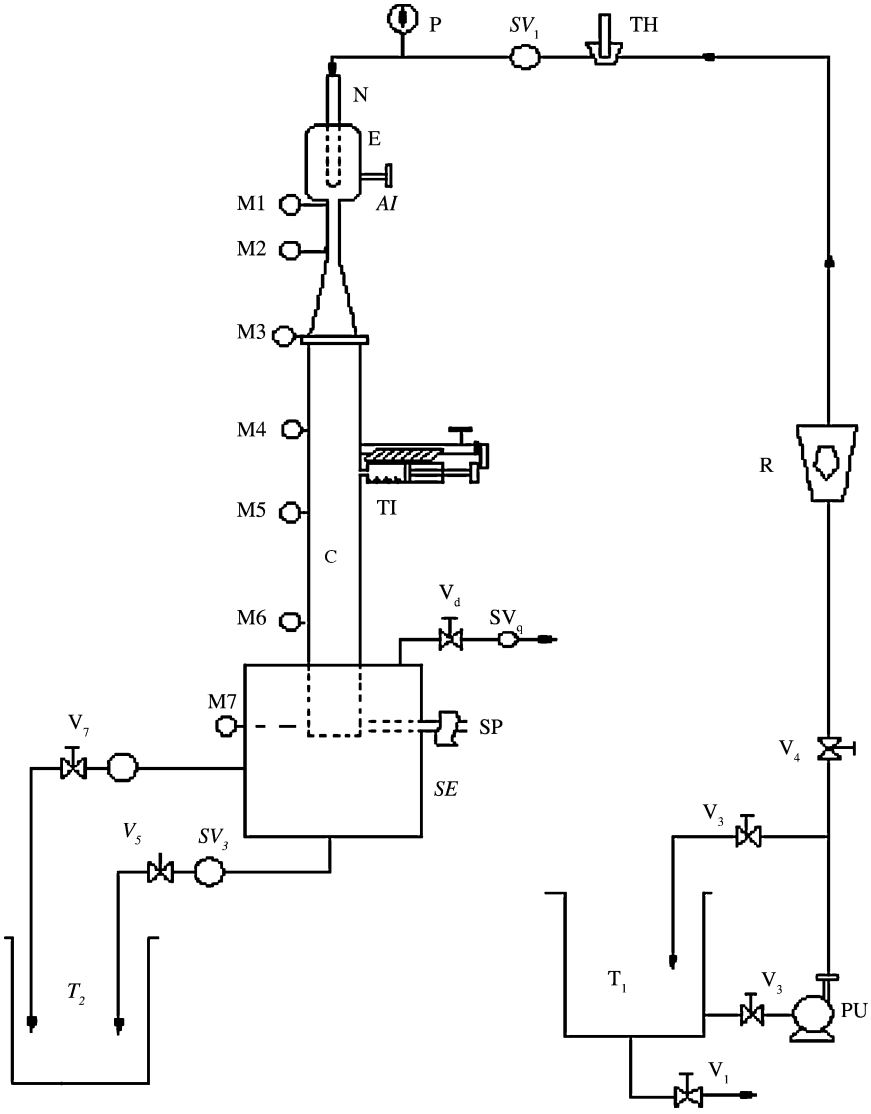

Fig. 2. Schematic diagram of experimental set-up. *Legend*—AI: air inlet; C: contactor; E: ejector; M_1–M_7: manometer ports; N: nozzle; P: pressure gauge; PU: pump; R: rotameter; SE: gas–liquid separator; SV_{1-4}: solenoid valves; SP: sampling port; T_1 and T_2: water tanks; TH: thermometer, TI: tracer inlet; V_1–V_7: control valves.

tively, and the constant k determined the form of velocity distribution. When the distribution is parabolic, k is equal to 768 [2]. In this work, we have applied the Taylor and Aris's model of homogeneous system to the ejector-induced downflow bubble column, because of well-homogenizing of two-phases in the column. To apply the above model in our system, the following assumptions have been made:

(i) The present bubble column is regarded as homogeneous [15].
(ii) Experimentally, it is observed that gas bubbles are dispersed uniformly. It follows a consequence that the dispersion coefficient due to bubble motion, D_b is uniform in the column and the contribution of D_b to the overall process is much larger than that of molecular diffusion.
(iii) Steady-flow condition is established in the longitudinal direction.

On the basis of the above assumptions, the dispersion coefficient in the bubble column was directly derived by replacing D_m in Eq. (6) with D_b.

$$E_z = \frac{D_c^2 V_0^2}{k D_b} + D_b \tag{7}$$

According to the Aris's [2] analysis, any definite value of local velocity can be used as the representative velocity V_0 in Eq. (7). In this analysis, we have used the following form of the representative velocity in the column:

$$V_0 = V_{L0} - V_{LW} \tag{8}$$

where V_{L0} is the interstitial liquid velocity in the centerline of the column and V_{LW} is the maximum interstitial liquid

velocity near the column wall. Interstitial liquid velocity is defined as $V_{SL}/(1-\varepsilon_G)$. Maximum interstitial velocity of the liquid are considered when the column diameter is large. In case of large column diameter, the local velocity V_0 varies due to variation of radial gas hold-up. In this present study, as the column diameter is small and for homogeneity of two-phases, assuming no radial change of interstitial velocity of the liquid across the column. Therefore, it is considered that liquid flows downward everywhere in the column and hence the interstitial liquid velocity at the centerline (V_{L0}) and at the wall (V_{LW}) are same at steady-state. Both of the velocities are equal to the interstitial liquid velocity (V_L) and it can be expressed as:

$$V_{L0} = -V_{LW} = V_L \tag{9}$$

Therefore, Eq. (8) can be expressed as:

$$V_0 = 2V_L \tag{10}$$

The effect of the profile of the velocity in the column can be modified by the coefficient k. The coefficient k is called characteristic factor of velocity distribution inside the column. Then, the dispersion coefficient is:

$$E_z = \frac{4D_c^2 V_L^2}{kD_b} + D_b \tag{11}$$

5.1. Experimental apparatus and technique

The schematic diagram of the experimental set-up is shown in Fig. 2. It consists of an ejector assembly; extended pipeline contactor, a gas–liquid separator and other accessories as mentioned in the legend. For visual observation of the flow and mixing patterns, the ejector assembly and extended contactors were made of perspex having 0.05 and 0.06 m internal diameter and 1.45 m length. The major dimensions of the apparatus are given in Table 1.

In the present set-up, the optimum dimensions of the ejector reported by Ref. [20] were used. The forcing nozzle is of the straight hole-type and is precision bored to obtain a smooth passage and to avoid any undue shock and losses. The dimensions of the nozzles used are given in Table 1.

An extended pipeline contactor was provided below the ejector assembly as shown in Fig. 2 for gas–liquid two-phase downflow. The lower end of the contactor projected 0.45 m into the separator. This arrangement enabled uniform movement of the two-phase downflow and easy separation of the bubbles from the main stream. The air–liquid separator was sufficiently large (0.41 m × 0.41 m × 0.86 m, mild steel vessel) to minimize the effect due to liquid going out of the separator or gas–liquid separation. There are three outlets provided at the top, bottom and center of the separator. The bottom and center outlets of the separator allowed the liquid to flow out while the top outlet allowed the gas to leave the separator. By operating the valves V_4–V_7 shown in Fig. 2, the liquid level inside the separator was maintained. The nozzle, the ejector assembly and the contactor were perfectly aligned in a vertical position to obtain an axially symmetric jet and the nozzle was fixed at the optimum position at a distance of one throat diameter from the entry of the throat. This distance was fixed on the basis of earlier experiments with horizontal and vertical liquid–gas system [6]. In an actual experiment, the jet is allowed to plunge into the liquid in the column. A level of liquid is maintained at a particular height by adjusting the pressure in the separator. After steady-state was reached and when the flow is fully developed [17,18], the tracer, 20 ml of potassium chloride solution of concentration, 40.0 kg/m^3 in water was injected at a point 30 cm below the top of the column, where the level of gas–liquid mixture crosses the level of injection. The volume of tracers used was kept small (1.0%) in relation to the total volume of the column [16,23]. The injection was carried out as quickly (0.5 s) and smoothly as possible by a high-pressure spring-loaded syringe. Liquid phase was sampled at every 3 s interval at the column exit by means of tubes. Variation of tracer concentration with time was measured by digital electrical conductivity meter [Model 601E, M.S. Electronic India Limited]. The experiments were conducted at liquid flowrates, 1.39×10^{-4} to 2.78×10^{-4} m^3/s and gas flowrates, 3.30×10^{-6} to 26.7×10^{-6} m^3/s. At constant liquid flowrate (Q_L), gas entrainment rates (Q_G) were varied by the control valve V_6 and maintaining constant liquid level by valves V_5 and V_7. At steady-flow of gas and liquid pressure readings were noted from the manometers connected to the column. Overall, gas hold-up for the present system was measured by phase-isolating method and from pressure drop. According to phase-isolating method, when a steady-state condition of the system was attained, the total height of gas–liquid mixture in the column was noted. Then, the three solenoid valves, SV_1–SV_3 (Fig. 2) were switched off simultaneously. This caused an immediate termination of flow of both the fluids. When the liquid–gas mixture inside the column got arrested the mixture was allowed to settle for some time, whereby all the gases got separated. The clear liquid height inside the column was then noted. The difference between the gas–liquid mixing height (H_0) and the corresponding clear liquid height (H) gave the overall gas hold-up in the column and calculated as $\varepsilon_G = (H_0 - H)/H_0$. The overall gas hold-up was calculated from the pressure difference as $\varepsilon_G = 1 - \Delta P/\rho_L g \Delta z$.

Table 1
Dimensions of the ejector-contactor assembly

Description	Dimension (mm)
Height of the suction chamber, h_s	50.0
Diameter of suction chamber, d_s	60.0
Diameter of throat, d_t	19.0
Length of the throat, L_t	183.0
Length of the diffuser, L_d	254.0
Diameter of the contactor, D_c	60.0
Diameter of gas inlet, d_i	10.0
Length of the contactor, L_c	1450.0
Diameter of the nozzle used, D_n	4–7

6. Results and discussion

The experimental results obtained show that the longitudinal dispersion coefficient is affected by the independent variables, such as nozzle diameter, superficial liquid velocity and superficial gas velocity is presented as follows.

6.1. Effect of nozzle diameter on longitudinal dispersion coefficient

As shown in Fig. 3, the longitudinal dispersion coefficient increases with decreasing nozzle diameter at constant superficial liquid velocity and constant superficial gas velocity. As the nozzle diameter decreases, jet velocity increases which enhances the turbulence of the phases in the column indicating that flow gets more agitated. The entrainment depth of the liquid jet increases as the nozzle diameter decreases which causes the increase of the size of the liquid circulation cells around the liquid jet in the column. This may also cause the increase of the dispersion coefficient as nozzle diameter decreases.

6.2. Effect of superficial liquid velocity on longitudinal dispersion coefficient

Increasing the convection transport, as characterized by the liquid superficial velocity V_{SL}, will increase the intensity of dispersion, as characterized by longitudinal dispersion coefficient. Joshi and Sharma [12] reported that the liquid-phase longitudinal dispersion in upward bubble column is independent of the superficial liquid velocity. However, they explained that in all the studies, the order of magnitude of the generated liquid circulation velocity is much higher than the superficial liquid velocity (at least by a factor of 10) resulting in weak dependence of the superficial liquid velocity on Peclet number as well as longitudinal dispersion coefficient. But in the case of ejector-induced downflow bubble column reactor, there is a significant influence of interstitial liquid velocity on the liquid dispersion. In this case, the longitudinal dispersion coefficient increases with increasing superficial liquid velocity at column diameter 0.06 m as shown in Fig. 4.

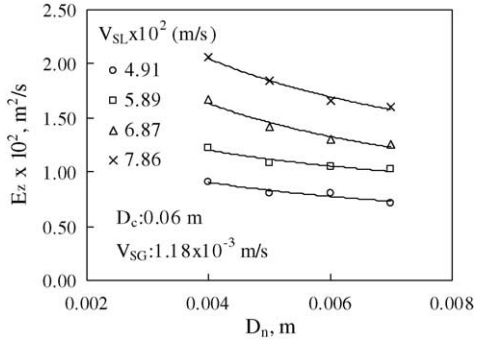

Fig. 3. Variation of longitudinal dispersion coefficient with nozzle diameter.

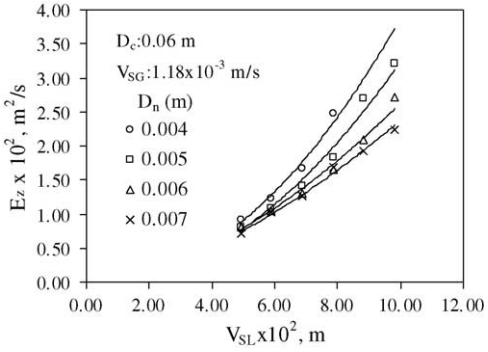

Fig. 4. Variation of longitudinal dispersion coefficient with superficial liquid velocity.

The greater extent of mixing at the higher superficial liquid velocity is probably because of more turbulence of liquid flow. Gas hold-up increases with increase in superficial liquid velocity. The intimate contact between the phases increases as gas hold-up increases which creates more turbulence in the column. This may result in increase of longitudinal dispersion coefficient with increase in superficial liquid velocity.

6.3. Effect of superficial gas velocity on longitudinal dispersion coefficient

The liquid-phase longitudinal dispersion is mainly because of the gas hold-up profile, which sets up along the column due to the tendency of gas bubbles to move down through the column [14,15]. At higher superficial liquid velocity, gas hold-up increases due to higher entrainment of the gas. As a result, the circulation and interaction of the gas and liquid phases increase inside the column and the flow gets more agitated. This enhances the overall mixing in the column. Fig. 5 shows that at constant nozzle diameter (0.007 m), the longitudinal dispersion coefficient increases with superficial gas velocity except $V_{SL} = 4.91 \times 10^{-2}$ m/s.At low superficial liquid velocity, the momentum transfer of the liquid jet is low for which the entrainment depth of the liquid jet is reduced and the hence fluid turbulence

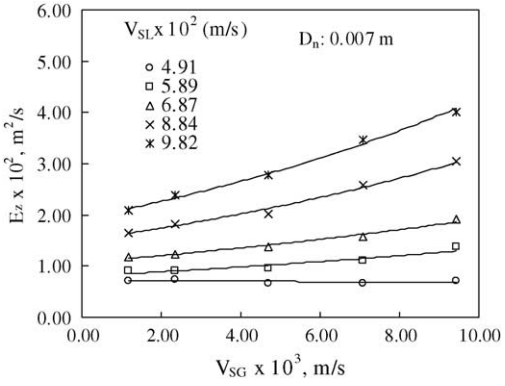

Fig. 5. Variation of longitudinal dispersion coefficient with superficial gas velocity.

inside the column decreases. This results the dispersion coefficient, E_z is nearly constant at low superficial liquid velocity.

7. Estimation of parameters, D_b and k

In order to calculate the dispersion coefficient by Eq. (11), the value of D_b, the coefficient k and the interstitial liquid velocity V_L must be known. The interstitial liquid and gas velocity was calculated as $V_L = V_{SL}/(1-\varepsilon_G)$ and $V_G = V_{SG}/\varepsilon_G$, respectively. The interstitial liquid velocity (V_L) in the column depends on fractional gas hold-up (ε_G), which contributes to the order of k and D_b (Eq. (11)). In the ejector-induced downflow bubble column, it is observed that ε_G is a function of V_G, V_j, D_n, D_c and H_0. Therefore, a correlation has been developed to obtain interstitial liquid velocity, V_L with the independent variables, V_G, V_j, D_n, D_c and H_0 as:

$$V_L = 27.6 V_G^{0.041} V_j^{1.278} D_n^{2.498} D_c^{-1.767} H_0^{0.626} \quad (12)$$

where the ranges variables are $7.68 \times 10^{-2} < V_L < 27.67 \times 10^{-2}$ m/s, $2.30 \times 10^{-3} < V_G < 22.39 \times 10^{-3}$ m/s; $3.61 < V_j < 17.68$ m/s. From the experimental data, it may be concluded that the form of interstitial liquid velocity distribution is approximately parabolic and it depends on interstitial gas velocity, column diameter, nozzle diameter gas–liquid mixing height and the liquid jet velocity. The correlation coefficient and overall standard error of Eq. (12) calculated and found to be 0.996 and 0.013. The calculated values of interstitial liquid velocity (V_L) from Eq. (12) are plotted against the experimental values and are shown in Fig. 6(a).

The distribution of V_L is represented in Fig. 6(b) as a function of V_G at $D_C = 0.05$ and 0.06 m and $D_n = 0.005$ m. Interstitial liquid velocity is plotted as the function of interstitial gas velocity.

It is seen from the experimental data that the interstitial liquid velocity decreases with the increase of interstitial gas velocity. Since interstitial gas velocity is calculated as $V_G = V_{SG}/\varepsilon_G$ which in overall effect of gas hold-up may results in decrease of interstitial liquid velocity with increase of interstitial gas velocity.

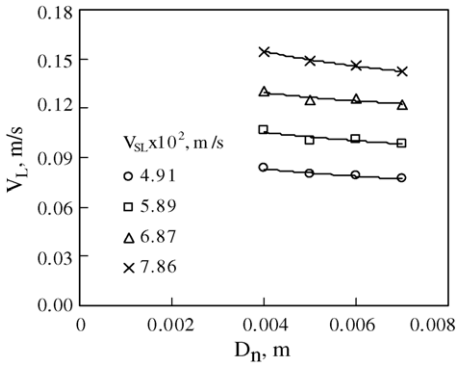

Fig. 7. Distribution of interstitial liquid velocity with nozzle diameter.

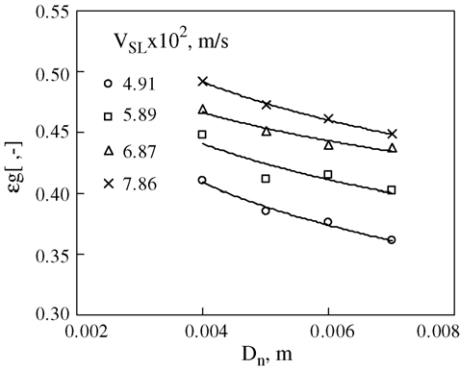

Fig. 8. Variation of fractional gas hold-up with nozzle diameter.

This may cause the approximately parabolic nature of interstitial liquid velocity with interstitial gas velocity. Fig. 7 shows that as the nozzle diameter increases the interstitial liquid velocity decreases. This is due to decrease of gas hold-up with increase in nozzle diameter. The variation of overall gas hold-up with nozzle diameter for different superficial liquid velocity is shown in Fig. 8.

Fig. 9 summarizes the comparison of overall gas hold-up calculated by isolated and pressure difference method. The

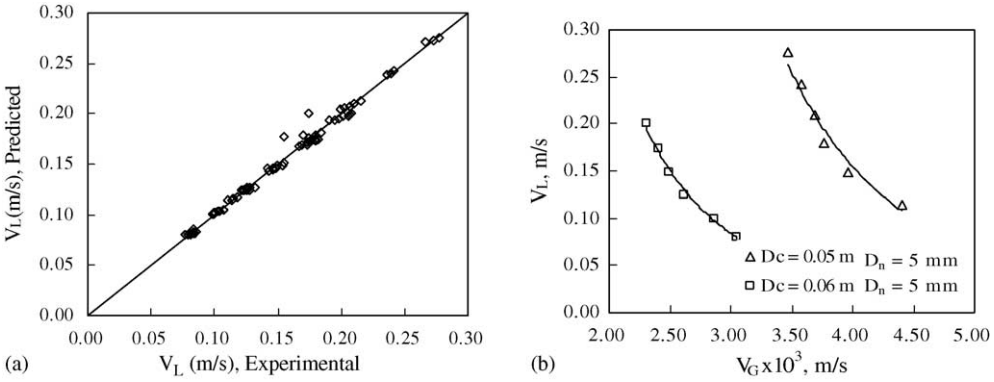

Fig. 6. (a) Comparison of the experimental values of interstitial liquid velocity (V_L) with that calculated from Eq. (12). (b) Distribution of interstitial liquid velocity with the interstitial gas velocity.

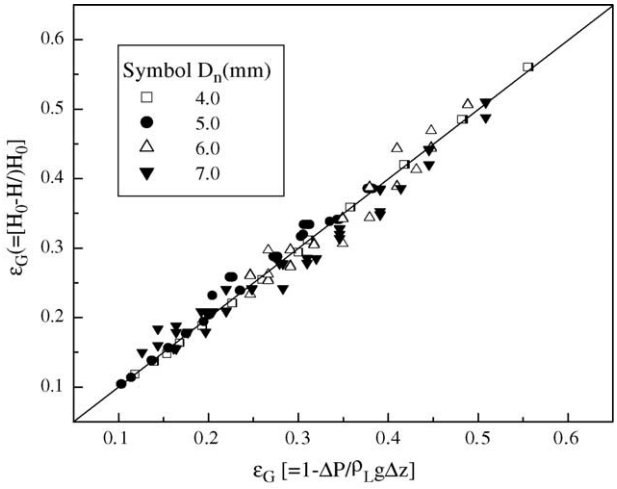

Fig. 9. Parity of fractional gas hold-up calculated by isolated and pressure difference methods.

standard deviation of the gas hold-up measured by these two methods is 0.113.

Now substituting V_L from Eq. (12) into Eq. (11), one gets:

$$E_z = \frac{V_G^{0.082} V_j^{2.556} D_n^{4.996} D_c^{-1.534} H_0^{1.252}}{3.28 \times 10^{-4} k D_b} + D_b \quad (13)$$

which can be written as:

$$E_z = \frac{X}{k D_b} + D_b \quad (14)$$

where

$$X = \frac{V_G^{0.082} V_j^{2.556} D_n^{4.996} D_c^{-1.534} H_0^{1.252}}{3.28 \times 10^{-4}} \quad (15)$$

According to Ohki and Inoue (1969), for co-current upward bubble column the form of equation is as follows:

$$E_z = \frac{576 D_c^2 V_G^{1.2}}{k D_b} + D_b \quad (16)$$

7.1. Comparison with experimental data

The validity of the velocity distribution model is examined by the comparison between the dispersion coefficients calculated by Eq. (13) and the experimental data. For the calculation of dispersion coefficient, it is necessary to decide the accurate values of k and D_b. These values are calculated from the slopes and intercepts of Eq. (14) by substituting the values measured at different experimental conditions into Eq. (14). Longitudinal dispersion coefficient E_z as a function of X for different nozzle diameter at $V_{SG} = 1.18 \times 10^{-3}$ m/s, $V_{SL} = 4.91 \times 10^{-2}$ to 9.82×10^{-2} m/s and $D_c = 0.06$ m is shown in Fig. 10. Therefore, predicted values of longitudinal dispersion coefficient can be obtained by putting the values of k and D_b in Eq. (14). The parity plots for the experimental dispersion coefficient and predicted dispersion coefficient using Eq. (14) are shown in Figs. 11 and 12 at

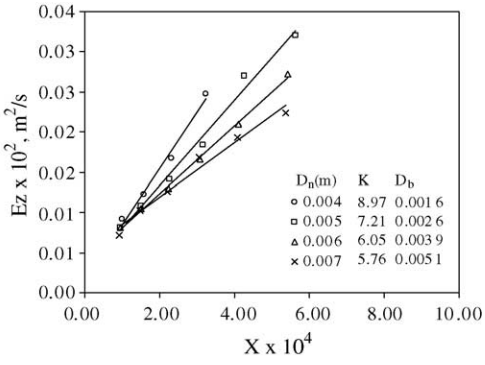

Fig. 10. Variation of longitudinal dispersion coefficient of liquid with X.

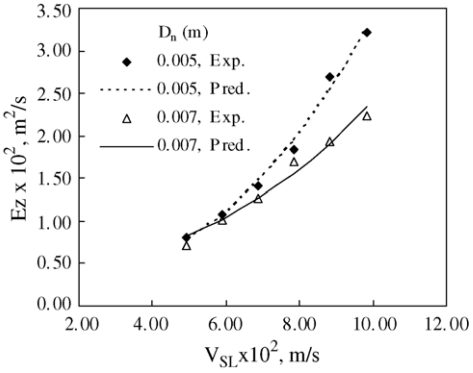

Fig. 11. Comparison of predicted longitudinal dispersion coefficient with experimental values varying superficial liquid velocity.

$V_{SG} = 1.18 \times 10^{-3}$ m/s and within the range of superficial liquid velocity, $V_{SL} = 4.91 \times 10^{-2}$ to 9.82×10^{-2} m/s and $D_c = 0.06$ m. It can be seen that the model can accurately predict the liquid longitudinal dispersion coefficient in the present bubble column experiments. By fitting Eq. (14) with experimental data for other different conditions, k and D_b can be calculated. The results are summarized in Tables 2 and 3. Ohki and Inoue (1969) found that D_b, the second term of Eq. (16) is very small and can be neglected in comparison to the first term. In the present system, it was also found that the values of D_b are very small compared to the values of first term of Eq. (13). Table 2 shows the calculated values of

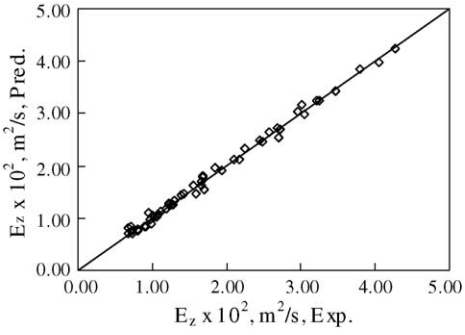

Fig. 12. Comparison of predicted longitudinal dispersion coefficient with experimental values.

Table 2
Variation of dispersion coefficient of bubble motion (D_b) and velocity profile coefficient (k) with diameter of nozzle (D_n)

D_n (m)	$V_{SG} \times 10^{-3}$ (m/s)	$D_b \times 10^3$ (m^2/s)	k (s/m^3)
0.004	1.18	1.60	8.97
0.005	1.18	2.60	7.21
0.006	1.18	3.90	6.05
0.007	1.18	5.10	5.76

Table 3
Variation of dispersion coefficient of bubble motion (D_b) and velocity profile coefficient (k) with superficial gas velocity (V_{SG})

D_n (m)	$V_{SG} \times 10^{-3}$ (m/s)	$D_b \times 10^3$ (m^2/s)	k (s/m^3)
0.007	1.18	5.10	5.76
0.007	2.36	3.20	7.21
0.007	4.71	2.30	8.58
0.007	7.07	1.50	11.50
0.007	9.43	1.20	12.82

dispersion coefficients of bubble motion (D_b) and velocity profile coefficient (k) calculated from experimental data at different nozzle diameters at constant $V_{SG} = 1.18 \times 10^3$ m/s and $V_{SL} = 4.91 \times 10^{-2}$ to 9.82×10^{-2} m/s.

The distribution is parabolic, k is equal to 768 [2] for upflow bubble column. In the present system, the values of k are much less than 768. It may be due to complex velocity distribution in downflow bubble column. Since the velocity distribution in the present downflow system is quite different than the upflow system, the mixing characteristics in the present system is quite different. In this present system, the turbulence of the fluid inside the column is much significant due to higher momentum transfer of the plunging liquid jet and higher gas hold-up. This may cause the greater effect of D_c and V_G on dispersion coefficient. The interstitial liquid velocity inside the column is a function of gas hold-up. As the fractional gas hold-up increases, the interstitial liquid velocity increases because the liquid hold-up decreases and hence causes the variation of D_b and k with nozzle diameter and superficial gas velocity. The coefficient of velocity profile decreases with increase in nozzle diameter at constant superficial gas velocity. This characterizes the different velocity profile for different nozzle diameters, which is accountable for variation of longitudinal dispersion coefficient. Table 3 shows the calculated value of dispersion coefficient of bubble motion, D_b and velocity profile coefficient, k calculated from experimental data at different superficial gas velocities with constant nozzle diameter within the same range of superficial liquid velocity.

It is seen that with increase in gas velocity, D_b decreases and k increases. The interstitial liquid velocity inside the column is a function of gas hold-up. As the fractional gas hold-up increases the interstitial liquid velocity inside the column increases because of decreasing flow area. This may results the variation of D_b and k with nozzle diameter and superficial gas velocity. From the experimental results, it is seen that the values of D_b and k vary with nozzle diameter, column diameter and the gas flowrates at the given range of operation limit of liquid flowrates [$V_{SL} = 4.91 \times 10^{-2}$ to 9.82×10^{-2} m/s]. Since there is no model or data available in literature for D_b and k, correlations have been developed with the above variables by dimensional analysis to obtain the values of D_b and k as follows:

$$D_b = 0.389 D_R^{1.68} Re_G^{-0.49}; \quad R^2 = 0.931, \quad \text{standard error}: \ 0.129 \tag{17}$$

and

$$k = 0.784 D_R^{-0.68} Re_G^{0.23}; \quad R^2 = 0.942, \quad \text{standard error}: \ 0.126 \tag{18}$$

Table 4
Comparison for axial dispersion coefficient in different bubble columns with the present work (E_z calculated based on the ranges of present work)

Types of bubble column with distributor	Systems; measuring method; tracer used	Equations for axial dispersion coefficient for different types of bubble column	$E_z \times 10^4$ (m^2/s)	Authors
UF, perforated plates	Air–water; pulse; dye	$E_z = 1.23 D_C^{1.5} V_{SG}^{0.5}$	6.21–17.6	[27]
UF, perforated plates	Air–water; pulse (mixing time)	$E_z = (0.065 + 0.3\, V_{SG}^{0.77}) D_C^{1.25} \mu_L^{-0.12}$	46.6–51.2	[11]
UF, nozzle, glass sintered porous plate	Air–water; aqueous solution of Na_2SO_3, NaCl; pulse; dye	$E_z = 0.68 D_C^{1.4} V_{SG}^{0.3}$	17.5–32.7	[7]
UF, liquid jet ejector	Air–water; pulse; NaCl	$E_z = 5.04 \times 10^{-2} \left(\frac{D_N}{D_T}\right)^{0.9} V_{SG}^{0.32} \left(\frac{V_{LT}^2}{g D_T}\right)^{-0.23}$	5.40–8.21	[21]
UF, sintered polyethylene porous plate	Air–water; LDA	$E_z = V_{SL} D_C$	29.5–82.1	[9]
Batch mode with no inflow or outflow of liquid, sintered bronze plate	Air–water; pulse, NaCl	$E_z = 0.0651 (g D_C)^{1/2} \left(\frac{V_{SG}}{g \upsilon_l}\right)^{1/8} D_C$	56.09–72.72	[13]
UF, nozzle-perforated plate	Air–water; pulse; $KMnO_4$	$E_z = 0.014 V_{SG}^{0.45} \exp(-48.85 V_{SL})$	0.087–3.10	[1]
Ejector-induced downflow bubble column	Air–water; pulse; KCl	$E_z = \frac{X}{k D_b} + D_b; \quad X = \frac{V_G^{0.082} V_j^{2.556} D_n^{4.996} D_c^{-1.534} H_0^{1.252}}{3.28 \times 10^{-4}}$	66.80–636.20	Present work

The above correlations have been made with the present experimental data, where $D_R = D_n/D_c$, $Re_G = D_c\rho_G V_{SG}/\mu_G$ within the ranges of $0.08 \leq D_R \leq 0.116$ and $5.30 \leq Re_G \leq 35.38$.

8. Comparison for longitudinal liquid dispersion coefficient in different co-current bubble column reactors with the present work

Numerous empirical correlations for longitudinal liquid dispersion coefficient have been published on bubble column. However, most of the empirical correlations are available on longitudinal liquid dispersion coefficient only for upflow bubble column with different types of distributor. A comparison between the present experimental results of the longitudinal liquid dispersion in ejector-induced downflow bubble column and a number of empirical correlations from the literature is shown in Table 4. The calculation for the longitudinal dispersion coefficients from different correlations has been done based on the ranges of superficial liquid velocity and superficial gas velocity of the present work. From this comparison, it can be seen that for the same ranges of the operating parameters, the liquid longitudinal dispersion coefficient of the present study is higher than the other mentioned studies. There is no relevant information regarding the mixing characteristics in the downflow bubble column, so a comparison has been made only with mixing intensity in upflow bubble column. From the comparison, it is seen that the performance of the present downflow system is better than the other upflow system. In the present, downflow bubble column higher momentum exchange of plunging liquid jet enhance the turbulence of liquid. This results the dispersion coefficient of liquid phase, E_z, in the downflow system is an order of magnitude much larger than that in the upflow.

9. Conclusion

From the experiment, it has been observed that the longitudinal dispersion coefficient of liquid in the ejector-induced downflow bubble column is strongly dependent on nozzle diameter and interstitial liquid and gas velocities. The longitudinal dispersion coefficient of liquid has been derived by the velocity distribution model based on Taylor's theory. The dispersion coefficient of bubble motion D_b and the characteristic factor of velocity distribution depend on different operating conditions, which give the corresponding model equations. The dispersion coefficients calculated from the model show a good agreement with the experimental data. It was also seen that the longitudinal dispersion coefficient of liquid in the present system is much higher than the other system. It implies that the mixing performance of the downflow bubble column with ejector system is better than the other type of bubble column.

Acknowledgement

The authors wish to acknowledge the Council of Scientific and Industrial Research, Human Resource Development Group, India, for financial support towards this project.

References

[1] T.S. Ahmad, Gas hold-up and liquid axial dispersion under slug flow conditions in gas–liquid bubble column, Chem. Eng. Process. 42 (10) (October 2003) 767–775.
[2] R. Aris, On the dispersion of a solute in a fluid through a tube, in: Proceedings of the Royal Society of London, vol. A235, 1956, p. 67.
[3] Y. Bando, M. Uraishi, M. Nishimura, M. Hattori, T. Asada, Cocurrent downflow bubble column with simultaneous gas–liquid injection nozzle, J. Chem. Eng. Jpn. 21 (1988) 607–612.
[4] A.K. Bin, Gas entrainment by plunging liquid jet, Chem. Eng. Sci. 48 (1993) 3585–3630.
[5] J.M. Burgess, N.A. Molloy, Gas absorption in plunging jet reactor, Chem. Eng. Sci. 28 (1973) 183–190.
[6] A.K. Datta, Effect of mixing throat length on the performance of a liquid jet ejector, M.Tech. Thesis, I.I.T. Kharagpur, India, 1976.
[7] W.D. Deckwer, R. Burckhart, G. Zoll, Mixing and mass transfer in tall bubble columns, Chem. Eng. Sci. 29 (11) (November 1974) 2177–2188.
[8] G.M. Evans, A.K. Bin, P.M. Machniewski, Performance of confined plunging liquid jet bubble column as a gas–liquid reactor, Chem. Eng. Sci. 56 (2001) 1151–1157.
[9] J.S. Groen, R.G.C. Oldeman, R.F. Mudde, H.E.A. van den Akker, Coherent structures and axial dispersion in bubble column reactors, Chem. Eng. Sci. 51 (10) (1996) 2511–2520.
[10] G. Hebrard, D. Bastoul, M. Roustan, M.P. Comte, C. Beck, Characterization of axial liquid dispersion in gas–liquid and gas–liquid–solid reactors, Chem. Eng. J. 72 (2) (February 1999) 109–116.
[11] H. Hikita, H. Kikukawa, Liquid-phase mixing in bubble columns: effect of liquid properties, Chem. Eng. J. 8 (1974) 191–197.
[12] J.B. Joshi, M.M. Sharma, A circulation cells model for bubble column, Trans. Inst. Chem. Eng. 57 (1979) 244–251.
[13] R. Krishna, M.I. Urseanu, J.M. Van Baten, J. Ellenberger, Liquid phase dispersion in bubble columns operating in the churn-turbulent flow regime, Chem. Eng. J. 78 (1) (July 2000) 43–51.
[14] A. Kulkarni, Y.T. Shah, Gas phase dispersion in a downflow bubble column, Chem. Eng. Commun. 28 (1983) 311–326.
[15] G. Kundu, D. Mukherjee, A.K. Mitra, Experimental studies on a cocurrent gas–liquid downflow bubble column, Int. J. Multiph. Flow 21 (5) (1995) 893–906.
[16] O. Levenspiel, W.K. Smith, Chem. Eng. Sci. 6 (1957) 227–233.
[17] A. Mandal, G. Kundu, D. Mukerjee, Interfacial area and liquid-side mass transfer coefficient in downflow bubble column, Can. J. Chem. Eng. 81 (2003) 212–219.
[18] A. Mandal, G. Kundu, D. Mukerjee, Gas-hold-up distribution and energy dissipation in an ejector-induced downflow bubble column: the case of non-Newtonian liquid, Chem. Eng. Sci. 59 (13) (July 2004) 2705–2713.
[19] S. Moustiri, G. Hebrard, S.S. Thakre, M. Roustan, A unified correlation for predicting liquid longitudinal dispersion coefficient in bubble columns, Chem. Eng. Sci. 56 (3) (2001) 1041–1047.
[20] D. Mukherjee, M.N. Biswas, A.K. Mitra, Hydrodynamics of liquid–liquid dispersion in ejectors and vertical two-phase flow, Can. J. Chem. Eng. 66 (1988) 896–907.
[21] S. Ogawa, M. Kobayashi, S. Tone, T. Otake, Liquid phase mixing in the gas–liquid jet reactor with liquid jet ejector, J. Chem. Eng. Jpn. 15 (6) (1982) 469–473.

[22] M.W. Peter, H. Herman, P.A. Frans, L.L. Stokman, V. Dierendonck, Liquid mixing in a bubble column under pressure, Chem. Eng. Sci. 48 (10) (1993) 1785–1791.
[23] T. Reith, S. Renken, B.A. Israël, Gas hold-up and axial mixing in the fluid phase of bubble columns, Chem. Eng. Sci. 23 (6) (August 1968) 619–629.
[24] U. Rustemeyer, J. Pauli, Th. Menzel, R. Buchholz, U. Onken, Liquid-phase mixing model for hydrodynamics of bubble columns, Chem. Eng. Process. 26 (2) (October 1989) 165–172.
[25] H.E. Sherif, K. Schügerl, Hold-up and backmixing investigations in co-current and countercurrent bubble columns, Chem. Eng. Sci. 30 (10) (October 1975) 1251–1256.
[26] G.I. Taylor, Dispersion of solute matter in solvent flowing slowly through a tube, in: Proceedings of the Royal Society of London, vol. A219, 1953, p. 186.
[27] G.D. Towell, G.H. Ackerman, Axial mixing of liquid and gas in large bubble reactors, in: Proceedings of the Fifth Europian/Second International Symposium, 1972, p. 31.
[28] G.Q. Yang, L.S. Fan, Axial liquid mixing in high-pressure bubble columns, AIChE J. 49 (8) (August 2003) 1995–2008.
[29] O. Yoshihiro, H. Inoue, Longitudinal mixing of the liquid phase in bubble columns, Chem. Eng. Sci. 25 (1969) 1–16.
[30] J. Zahradník, M. Fialová, The effect of bubbling regime on gas and liquid phase mixing in bubble column reactors, Chem. Eng. Sci. 51 (10) (May 1996) 2491–2500.